Chinese Chemical Letters 31 (2020) 1188–1192

Contents lists available at ScienceDirect

Chinese Chemical Letters

journal homepage: www.elsevier.com/locate/cclet

Communication

Stable deep blue organic light emitting diodes with CIE of $y < 0.10$ based on quinazoline and carbazole units

Bowen Li[a], Xiang'an Song[a], Xi Jiang[a], Zhiyi Li[b], Fengyun Guo[a], Ying Wang[b,**], Liancheng Zhao[a], Yong Zhang[a,c,*]

[a] School of Materials Science and Engineering, Harbin Institute of Technology, Harbin 150001, China
[b] Key Laboratory of Photochemical Conversion and Optoelectronic Materials, Technical Institute of Physics and Chemistry, Chinese Academy of Sciences, Beijing 100190, China
[c] School of Materials Science and Engineering, Zhengzhou University, Zhengzhou 450001, China

ARTICLE INFO

Article history:
Received 19 April 2019
Received in revised form 30 May 2019
Accepted 18 June 2019
Available online 18 June 2019

Keywords:
Organic light-emitting diodes
Deep blue emitter
Quinazoline
Carbazole
Electroluminescence

ABSTRACT

Achieving stable deep blue organic light emitting diodes (OLEDs) with narrow full width at half maximum (FWHM) and color gamut in the range of the commission International de L'Eclairage (CIE) of $y \leq 0.10$ is still challenging in display and lighting applications. In this investigation, three donor-acceptor (D-A) deep-blue emitters were designed and synthesized *via* integrating asymmetric quinazoline (PQ) acceptor with weak donating carbazole (Cz) donor. The effect of the position and number of Cz group in PQ unit are investigated, which is also first examples for systematic research about the effect of different position of asymmetric PQ as acceptor on deep OLEDs. Their bandgaps of 3.12∼3.19 eV and the singlet state energy levels of 3.12∼3.19 eV were found to be sufficiently large to achieve deep blue light. As expected, these emitters-based OLEDs exhibit deep blue emission with the maximum wavelength ≤ 450 nm and narrow FWHM ≈ 60 nm. Especially, a CIE of $y = 0.080$ was achieved for 4PQ-Cz-based OLED. Significantly, the deep blue electroluminescence (EL) spectra of these three emitters-based OLEDs are very stable and the corresponding CIE coordinates deviation (ΔCIE (x, y)) can be negligible under the applied voltage ranging from 5 V to 9 V.

Since the invention of organic light emitting diodes (OLEDs) by Tang *et al.* in 1987 [1], they have attracted a great deal of attention because of the many advantage of flexibility, image quality and contrast, and faster response times [2–7]. Although OLEDs have been commercialized in the mobile phone, such as the fold-screen Huawei Mate X, and displaying, the development of new red, green, and blue-emitter is still essential, especially deep blue emitting materials with CIE of $y \leq 0.10$ [8–12]. Common properties, such as high efficiency, blue emission with maximum wavelength ≤ 450 nm, and narrow FWHM ≤ 60 nm, are usually required for excellent blue emitters [2]. Up to now, much efforts in blue emitters are focused on the development of high efficient phosphorescent and thermally activated delayed fluorescent (TADF) materials owing to the possibility to harvest a theoretical internal quantum efficiency (IQE) of 100% [13–17], unfortunately, the phosphorescent and TADF OLEDs hardly fall into the deep blue region with CIE of $y \leq 0.10$ [18,19], or even ≤ 0.08 [16]. In addition, they often suffer from the poor color purity, high cost, and unstable EL spectra under the applied voltages [2,15], which severely limited the development of deep blue emitters. Therefore, it is essential to develop new stable deep blue emitting materials with CIE of $y \leq 0.10$, and to further extend deep blue materials family.

Quinazolines are heterocyclic aromatic molecules containing two nitrogen atoms and possess appropriate electron accepting ability [20]. Its derivatives are ubiquitous in a variety of natural products as well as synthetic pharmaceuticals, and have been widely investigated and used in medicinal applications, such as being as antimalarial and anticancer agents, *etc.* [21]. However, rare of the quinazoline derivatives are applied so far in OLEDs. Specifically, to our best knowledge, only limited numbers of quinazoline derivatives have been introduced into OLEDs as host for red and orange phosphorescent OLEDs [14,22]. Recently, we first introduced quinazoline as acceptor to TADF emitters and achieved the promising maximum external quantum efficiency (EQEs) over 20%, and showed that quinazoline is excellent acceptor

* Corresponding author at: School of Materials Science and Engineering, Harbin Institute of Technology, Harbin 150001, China.
** Corresponding author.
E-mail addresses: wangy@mail.ipc.ac.cn (Y. Wang), yongzhang@hit.edu.cn (Y. Zhang).

https://doi.org/10.1016/j.cclet.2019.06.033
1001-8417/

moiety for D-A type emitters [20]. However, these quinazoline-based emitters exhibit green to green-yellow EL owing to the lower singlet state energy (S_1) level of below than 2.51 eV.

Considering the S_1 energy level can easily adjust by changing the donating electronic ability of donor in D-A type emitters. In this paper, we select carbazole (Cz) as the weak donor and develop three quinazoline-based emitters, 9-(4-(2-phenylquinazolin-4-yl) phenyl)-9*H*-carbazole (2PQ-Cz), 9-(4-(4-phenylquinazolin-2-yl) phenyl)-9*H*-carbazole (4PQ-Cz) and 9,9′-(quinazoline-2,4-diylbis (4,1-phenylene))bis(9*H*-carbazole) (24PQ-Cz). We systematically investigate the effect of the substituted position and number of Cz in PQ unit on the photophysical and electroluminescent properties. It is found that these emitters have wide bandgaps of 3.12∼3.19 eV and large S_1 energy levels of 3.12∼3.19 eV, which is sufficiently large to achieve deep blue emission. As expected, these emitters-based OLEDs exhibit deep blue emission with the maximum wavelength $\leq$ 450 nm and narrow FWHM $\approx$ 60 nm. Significantly, the deep blue EL spectra of these emitters-based OLEDs are very stable and the corresponding ΔCIE (x, y) can be negligible under the applied voltage ranging from 5 V to 9 V. Additionally, these emitters are also the first examples using quinazoline as acceptor to achieve stable, high purity color, and deep blue emission with the maximum wavelength $\leq$ 450 nm and $y < 0.10$.

The synthetic routes for 2PQ-Cz, 4PQ-Cz, and 24PQ-Cz are showed in Scheme 1, the details are showed in the Supporting information. The *N*-phenyl-carbazole boronic ester was prepared according to our previous work [23]. The emitters 2PQ-Cz, 4PQ-Cz, and 24PQ-Cz were then synthesized through Pd-catalyzed Suzuki-Miyaura coupling reaction of **2** with 4-chloro-2-phenylquinazoline (2PQ-Cl), 2-chloro-4-phenylquinazoline (4PQ-Cl) and 2,4-dichloroquinazoline (24PQ-Cl), respectively. They were purified using column chromatography on silica gel, and further purified by temperatures-gradient sublimation under vacuum. The structure of the final product was confirmed by ^{1}H NMR, ^{13}C NMR, and mass spectrometry (Figs. S1-S9 in Supporting information). In addition, the thermal properties were characterized by thermogravimetric analysis (TGA) and differential scanning calorimetry (DSC) in nitrogen atmosphere. As shown in Fig. S10 (Supporting information), 2PQ-Cz, 4PQ-Cz, and 24PQ-Cz display excellent thermal stability with the decomposition temperature of 371, 375 and 468 °C, respectively, which are good enough for application in electroluminescent device.

To understand the electronic properties of three emitters 2PQ-Cz, 4PQ-Cz, and 24PQ-Cz, we utilized density functional theory (DFT) in Gaussian 09 at B3LPY/6-31 G(d) level to optimize the ground-state geometries and HOMO/LUMO. Since PQ moiety has an asymmetric structure, the connecting position of Cz may endow different twist angles between Cz donor and PQ acceptor. As shown in Fig. 1, it can be found that the optimized molecular geometrics of 2PQ-Cz show a dihedral angle of 40.5° between PQ moiety and phenyl spacer. However, for 4PQ-Cz, the dihedral angle decreases to 1.9° because of the absence of steric hindrance between nitrogen and hydrogen atoms. In addition, in the case of 24PQ-Cz, the dihedral angles between PQ moiety and phenyl spacer are 44.8° and 2.2°, respectively, which are similar to 2PQ-Cz and 4PQ-Cz. The different molecular geometrics of three emitters result various electron cloud distribution. For 2PQ-Cz, the HOMO is mainly located on Cz moiety and phenyl spacer, while the LUMO is mainly distributed on PQ moiety, phenyl spacer, and small portion spreading onto Cz moiety, resulting a lager orbital overlap of HOMO and LUMO on phenyl spacer. Due to the small twist angle between PQ moiety and phenyl spacer, the HOMO of 4PQ-Cz has a broader distribution over Cz with a part distribution on PQ. Similarly, the LUMO only distributed on PQ moiety and phenyl spacer compared to 2PQ-Cz. This result indicates that 2PQ-Cz has deeper HOMO and LUMO levels than 4PQ-Cz, which is consistent with the values of theoretical calculation. For 24PQ-Cz, the distribution of LUMO can be considered the combination of 2PQ-Cz and 4PQ-Cz, resulting a deeper LUMO level of −2.12 eV (−2.01 eV for 2PQ-Cz and −2.00 eV for 4PQ-Cz). While the HOMO distribution in 24PQ-Cz is more like HOMO of 4PQ-Cz, and the HOMO of 24PQ-Cz is calculated to be −5.28 eV, which is very close to −5.25 eV for 4PQ-Cz.

The experimental HOMO energy levels of three emitters are measured at anhydrous dichloromethane by cyclic voltammetry. It can find that each molecule exhibited a reversible oxidation wave (Fig. S11 in Supporting information). The HOMO energy levels were calculated from the onset of oxidation potential and were found to be −5.72 eV, −5.68 eV and −5.32 eV, respectively, for 2PQ-Cz, 4PQ-Cz, and 24PQ-Cz (Table 1). The LUMO energy levels were at −2.55 eV, −2.49 eV and −2.20 eV, respectively, which were calculated from the optical bandgap (E_g) from the HOMO energy levels. Similar energies splitting determined experimentally using $\Delta E_{ST} = E_S - E_T$ to DFT calculations, the higher HOMO and LUMO

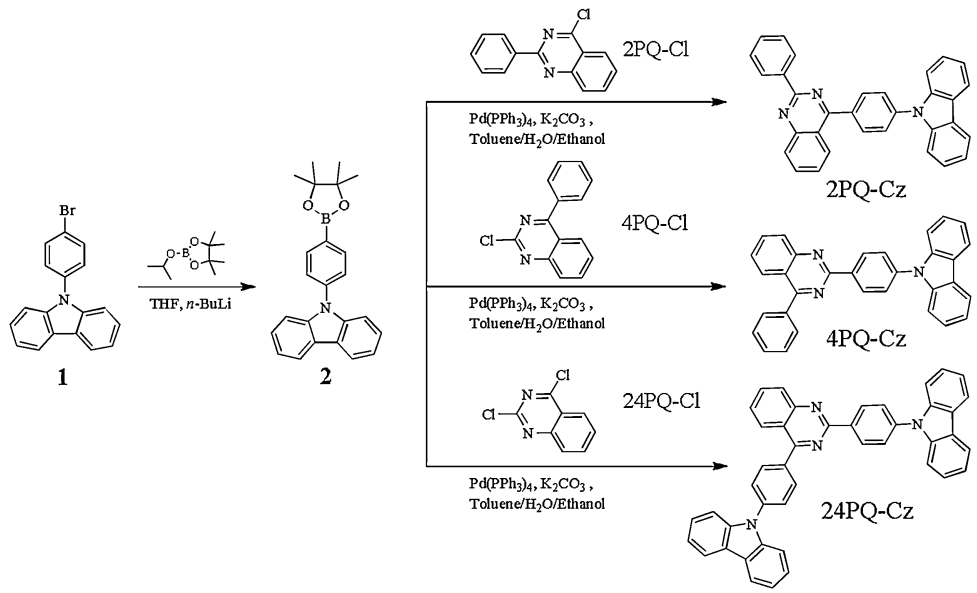

Scheme 1. Synthesis procedures of 2PQ-Cz, 4PQ-Cz and 24PQ-Cz.

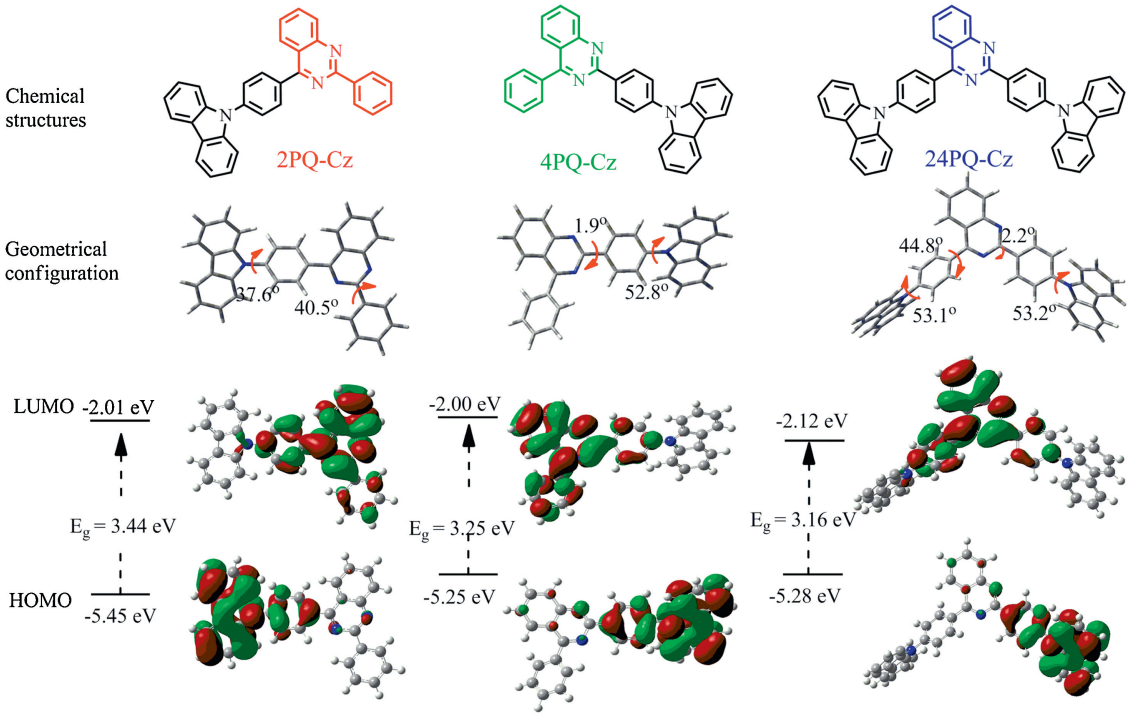

Fig. 1. Chemical structures, HOMO and LUMO distributions for 2PQ-Cz, 4PQ-Cz, and 24PQ-Cz based on TD-DFT at the B3LYP/6-31 G(d) level.

Table 1
The HOMO, LUMO, E_g, E_S, E_T and ΔE_{ST} values of 2PQ-Cz, 4PQ-Cz, and 24PQ-Cz.

Compounds	λ_{PL}[a]/ λ_{PL}[b] (nm)	HOMO[c] (eV)	LUMO[d] (eV)	E_g[e] (eV)	E_S[f] (eV)	E_T[g] (eV)	ΔE_{ST}[h] (eV)
2PQ-Cz	439/450	−5.72	−2.55	3.17	3.12	2.56	0.56
4PQ-Cz	425/442	−5.68	−2.49	3.19	3.19	2.53	0.63
24PQ-Cz	437/454	−5.32	−2.20	3.12	3.12	2.52	0.60

[a] Maximum wavelength of emission measured at toluene solution.
[b] Maximum wavelength of emission measured at neat film.
[c] HOMO were calculated from the oxidation potential.
[d] LUMO were calculated using HOMO-E_g.
[e] E_g was obtained from the absorption edges of normalized absorption spectra in toluene (1×10^{-4} mol/L).
[f] Estimated from the onset of fluorescence spectrum in toluene (1×10^{-4} mol/L) at 300 K.
[g] Estimated from the onset of phosphorescence spectrum in toluene (1×10^{-4} mol/L) at 77 K.
[h] Singlet-triplet.

energy levels of 24PQ-Cz compared to that of 2PQ-Cz and 4PQ-Cz is mainly stem from the special asymmetric D-A-D structure. These results indicated that the asymmetric D-A-D structure plays an important role on tuning the HOMO and LUMO energy levels, which are crucial for facilitating hole and electron injections in organic electroluminescent device.

The UV–vis absorption and photoluminescence (PL) spectra of 2PQ-Cz, 4PQ-Cz, and 24PQ-Cz in dilute toluene (10^{-4} mol/L) and neat film are showed in Fig. 2. It can find that these emitters exhibit similar absorption profiles and have an absorption shoulder between 350–412 nm, which is attributed to the intramolecular charge transfer (ICT) state between PQ unit and Cz moiety. The molar extinction coefficient of CT transition was measured to be 1.04×10^4, 1.22×10^4, 1.99×10^4 L mol^{-1} cm^{-1} for 2PQ-Cz, 4PQ-Cz, and 24PQ-Cz, respectively, suggesting that 2PQ-Cz has a weaker ICT interaction than 4PQ-Cz and 24PQ-Cz. A slight red-shift in the CT absorption edge was observed for 24PQ-Cz when compared with 2PQ-Cz, 4PQ-Cz, which likely ascribe to the expanded conjugation of 24PQ-Cz. Moreover, the E_g of 24PQ-Cz was calculated to be 3.15 eV, similar with the values of 2PQ-Cz

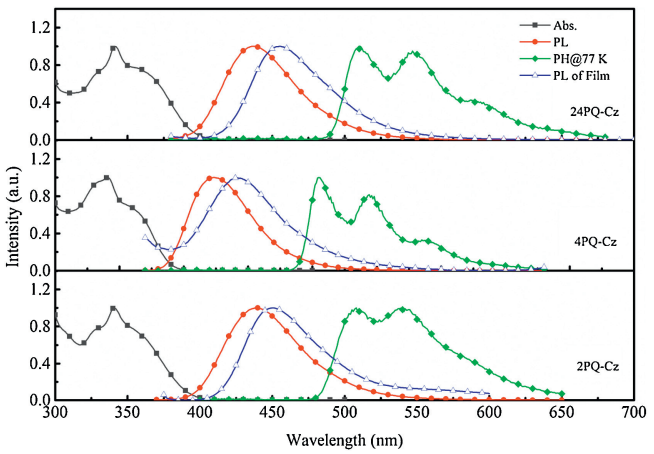

Fig. 2. UV–vis absorption, PL spectra in toluene solution (10^{-4} mol/L) and in neat film at room temperature and PH spectra in toluene solution at 77 K of 2PQ-Cz, 4PQ-Cz, and 24PQ-Cz.

(3.17 eV), 4PQ-Cz (3.19 eV), which suggests that the expanded conjugation has no obvious influence for emission in this type molecules, and the large E_g values of over 3.0 eV show a blue emission. As expect, the PL spectra in toluene of 2PQ-Cz, 4PQ-Cz, and 24PQ-Cz showed the intense blue emission with peaks at 423 nm, 438 nm and 439 nm, respectively. Due to the weak ICT character, the emission peak of 2PQ-Cz shows blue-shifted compared with 4PQ-Cz and 24PQ-Cz, which is similar with others reports [17,20]. Additionally, the PL spectra of 2PQ-Cz, 4PQ-Cz, and 24PQ-Cz in the neat film are slightly red-shifted compared with solution state, which should be attributed to the decreased polarity of neat film relative to toluene solvent [24]. It is well known that the solvent polarity has an effect on the optical properties of the organic light materials. As shown in Fig. S2, the absorption spectra of 2PQ-Cz, 4PQ-Cz, and 24PQ-Cz have almost no change in various polar solvents indicating the nonpolar ground states [23,25]. In contrast, the PL spectra of the three PQ-based emitters exhibited strong dependence on the solvent polarity (Fig. S12 and Table S1 in Supporting information). 2PQ-Cz, 4PQ-Cz, and 24PQ-Cz, respectively, with increasing polarity of solvents from *n*-hexane to DCM. These results also clearly indicate that the emissions of the three PQ-based emitters are from the ICT states with a more polar than the ground state. In addition, we also measured the low-temperature phosphorescence (PH) of 2PQ-Cz, 4PQ-Cz, and 24PQ-Cz in toluene at 77 K. It is found that PH spectra display similar vibronic structure, from which the triplet energy levels (E_T) are estimated to be 2.56, 2.53, 2.52 eV, respectively (Table 1). The E_Ts of three compounds are exactly similar to its acceptor moiety of 2-phenylquinazoline (E_T = 2.48 eV) [20], which indicate that the lowest triplet states of these compounds are local triplet states and derives from its acceptor. The large singlet-triplet energy gaps of 0.56, 0.63, 0.60 eV for 2PQ-Cz, 4PQ-Cz, and 24PQ-Cz, respectively, suggests that the reverse intersystem crossing process is largely forbidden, which confirmed by Fig. S13 (Supporting information) [8,20,23].

To evaluate device performances of 2PQ-Cz, 4PQ-Cz, and 24PQ-Cz, multilayer OLEDs were fabricated using thin film of these three PQ-based emitters in a high triplet energy DPEPO host as an emitting layer (EML). The device architecture, chemical structure of all materials, and energy level used in the OLEDs device are illustrated in Fig. 3a. The detailed device architectures are as following: glass substrate/ITO anode/ HATCN (5 nm)/TAPC (30 nm)/mCP (10 nm)/emitters: DPEPO (*x*) wt% (40 nm)/ DPEPO (5 nm)/TPBi (40 nm)/LiF (0.9 nm)/Al (100 nm). Among them, 2,3,6,7,10,11-hexacyano-1,4,5,8,9,12-hexaazatriphenylene (HATCN) and di-[4-(*N*,*N*-ditoly-amino)-phenyl]cyclohexane (TAPC) were used as a hole injection layer and a hole transporting layer, respectively. 1,3,5-Tris(*N*-phenylbenzimidazol-2-yl)benzene (TPBi) and LiF were the electron transporting layer and an electron injection layer, respectively. *N*,*N*-dicarbazolyl-3,5-benzene (mCP) and (oxybis(2,1-phenylene))bis(diphenylphosphine oxide) (DPEPO) were inserted as excitons blocking layer.

Through doping concentration optimization (10, 20, 30, 40, 50, 60 wt%), it is found that the doped OLEDs have the better EL properties at the doped concentration of 40 wt% in DPEPO (Figs. S14-S16 in Supporting information). All the optimized 2PQ-Cz-, 4PQ-Cz- and 24PQ-Cz-based devices exhibit turn-on voltages of 4.3, 4.3 and 3.9 V, and maximum luminance of 1668, 936, and 3850 cd/m^2, respectively (Table 2). The optimized 2PQ-Cz-based device delivered maximum external quantum efficiency of 2.17% (Fig. S17 and Table S2 in Supporting information). It is noteworthy that the OLED based on 2PQ-Cz displayed deep blue emission peak at 445 nm (Fig. 3b), with CIE coordinates of (0.152, 0.099). As discussed above, the asymmetric structure of quinazoline acceptor provides a possibility to modulate the luminescence properties. As it can see from Fig. 3c, the EL spectrum of 4PQ-Cz based OLEDs show deep blue emission peak at 436 nm with CIE coordinates of (0.157, 0.080), which is very close to the standard blue CIE values of (0.14, 0.08). To date, deep blue OLEDs with $y \leq 0.08$ as emitter are very rare. Therefore, the excellent EL spectrum and CIE of 4PQ-Cz-based OLEDs extend the deep blue emitters family. The maximum external quantum efficiency of 4PQ-Cz-based device is 1.33%. Compared to these two D-A emitters, the asymmetry D-A-D 24PQ-Cz exhibits a better EL properties and afford a EQE of 2.64%. However, the CIE of y is large 0.10, which is due to a larger conjugate length.

It is known that color purity is an important parameter for good color quality in display for OLED. Generally, emitters with classical charge-transfer excited states often display broad emission spectra and poor color purity [8]. It is notably that the EL spectra of 2PQ-

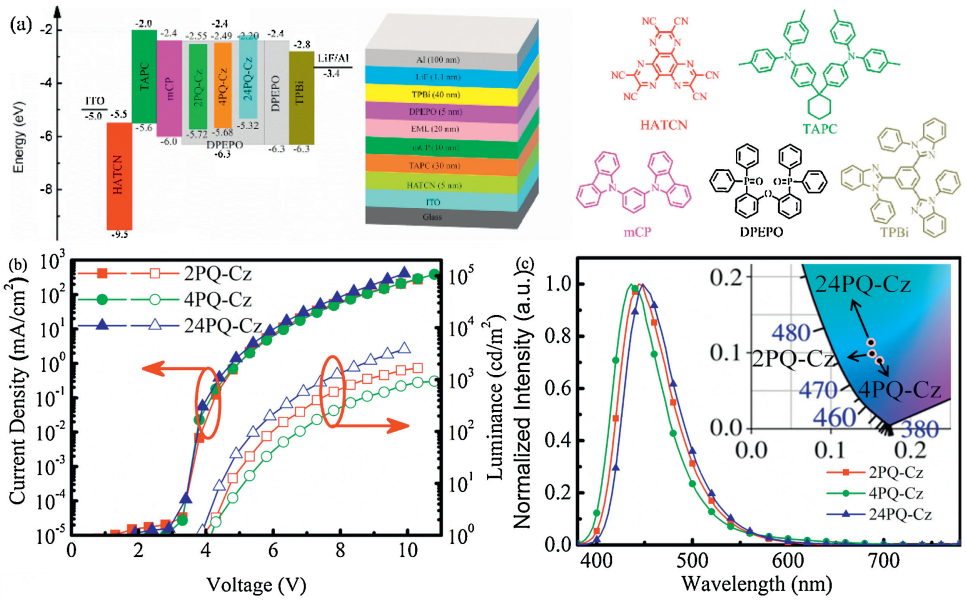

Fig. 3. (a) The energy level diagrams, OLED structure, and the chemical structure of the materials used in the TADF devices. Performance of 2PQ-Cz-, 4PQ-Cz- and 24PQ-Cz-based OLED with doped concentration of 40% in DPEPO. (b) Current density and luminance *versus* voltage (*J-V-L*) characteristics. (c) EL spectra of the TADF OLEDs at 7 V.

Table 2
Summary of OLED performances using 2PQ-Cz, 4PQ-Cz and 24PQ-Cz as dopants.

Emittes	λ_{EL}[a] (nm)	FWHM[b] (nm)	V_{on}[c] (V)	EQE_{max}[d] (%)	L_{max}[e] (cd/m^2)	CIE (x, y) [a]	ΔCIE (x, y) [f]
2PQ-Cz	445	63	4.3	2.17	1668	(0.152, 0.099)	(0.000, 0.002)
4PQ-Cz	436	61	4.3	1.33	936	(0.157, 0.080)	(0.003, 0.005)
24PQ-Cz	448	57	3.9	2.64	3850	(0.151, 0.113)	(0.001, 0.003)

[a] Measured at 7 V.
[b] Full width at half maximum.
[c] Turn-on voltage at 1 cd/m^2.
[d] Maximum external quantum efficiency.
[e] Maximum luminance.
[f] CIE coordinates deviation.

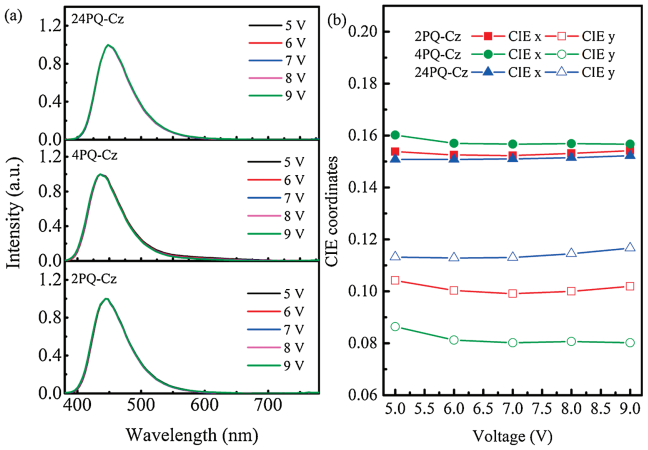

Fig. 4. (a) EL spectra of 2PQ-Cz-, 4PQ-Cz-, and 24PQ-Cz-based OLED from 5 V to 9 V. (b) CIE coordinates deviation of 2PQ-Cz-, 4PQ-Cz- and 24PQ-Cz-based OLEDs from 5 V to 9 V.

Cz-, 4PQ-Cz- and 24PQ-Cz-based OLEDs have narrow FWHM of 63, 61 and 57 nm, respectively. More importantly, EL spectra and CIE of these three emitters based OLEDs are almost completely consistent ranging from 5 V to 9 V, which indicate that the deep blue EL emissions are fairly stable under the applied voltage range (Fig. 4a). Furthermore, the corresponding ΔCIE (*x*, *y*) of (0.000, 0.002), (0.003, 0.005) and (0.001, 0.003) can be negligible for 2PQ-Cz-, 4PQ-Cz- and 24PQ-Cz-based OLEDs, respectively (Fig. 4b).

In conclusion, we have developed three new deep blue emitters, namely, 2PQ-Cz, 4PQ-Cz and 24PQ-Cz, by connecting quinzonline acceptor with carbazole donor. Their bandgaps of 3.17, 3.19, 3.12 eV are found to be sufficiently large to achieve deep blue light, responding the singlet state energy levels of 3.12, 3.19 and 3.12 eV, respectively. These emitters-based OLEDs exhibit deep blue emission with the maximum wavelength $\leq$ 450 nm and narrow FWHM $\approx$ 60 nm. Especially, a CIE of y = 0.080 is achieved for 4PQ-Cz-based OLED. This result indicates that the asymmetric quinazoline as acceptor not only can achieve deep blue materials for OLED, but also can effectively modulate the luminescence properties. Moreover, EL spectra and CIE of these three emitters based OLEDs are almost completely consistent ranging from 5 V to 9 V, which indicate that the deep blue EL emissions are fairly stable under the applied voltage range. The corresponding ΔCIE (*x*, *y*) of (0.000, 0.002), (0.003, 0.005) and (0.001, 0.003) can be negligible for 2PQ-Cz-, 4PQ-Cz- and 24PQ-Cz-based OLEDs, respectively.

Acknowledgments

The authors thank the supports from the National Key Research and Development Plan (No. 2016YFB0401004). Y. Zhang thanks the supports from the Open Fund of Beijing National Laboratory for Molecular Sciences (BNLMS, No. BNLMS20160131) and the Fundamental Research Funds for the Central Universities (Harbin Institute of Technology).

Appendix A. Supplementary data

Supplementary material related to this article can be found, in the online version, at doi:https://doi.org/10.1016/j.cclet.2019.06.033.

References

[1] C.W. Tang, S.A. VanSlyke, Appl. Phys. Lett. 51 (1987) 913–915.
[2] S. Kim, B. Kim, J. Lee, et al., Mater. Sci. Eng. R 99 (2016) 1–22.
[3] M.Y. Wong, E. Zysman-Colman, Adv. Mater. 29 (2017) 1605444.
[4] L. Gan, Z. Xu, Z. Wang, et al., Adv. Funct. Mater. (2019) 1808088.
[5] S. Chen, J. Lian, W. Wang, et al., J. Mater. Chem. C 6 (2018) 9363–9373.
[6] Y. Xu, X. Liang, X. Zhou, et al., Adv. Mater. 31 (2019) e1807388.
[7] Y. Xiong, J. Zeng, B. Chen, et al., Chin. Chem. Lett. 30 (2019) 592–596.
[8] Z. Li, C. Li, Y. Xu, et al., J. Phys. Chem. Lett. 10 (2019) 842–847.
[9] X. Xu, X. Li, S. Wang, et al., J. Mater. Chem. C 6 (2018) 9599–9606.
[10] W. Sun, N. Zhou, Y. Xiao, et al., Dye. Pigment. 154 (2018) 30–37.
[11] Y.X. Zhang, Y. Yuan, Q. Wang, et al., Dye. Pigment. 158 (2018) 396–401.
[12] H. Park, J. Lee, I. Kang, et al., J. Mater. Chem. 22 (2012) 2695–2700.
[13] N. Jürgensen, A. Kretzschmar, S. Höfle, et al., Chem. Mater. 29 (2017) 9154–9161.
[14] Z. Zhang, J. Xie, H. Wang, et al., Dye. Pigment. 125 (2016) 299–308.
[15] D.H. Ahn, S.W. Kim, H. Lee, et al., Nat. Photon. 13 (2019) 540–546.
[16] J. Lee, H.F. Chen, T. Batagoda, et al., Nat. Mater. 15 (2015) 92–98.
[17] K. Nakao, H. Sasabe, R. Komatsu, et al., Adv. Opt. Mater. 5 (2017) 1600843.
[18] R. Komatsu, T. Ohsawa, H. Sasabe, et al., ACS Appl. Mater. Interfaces 9 (2017) 4742–4749.
[19] J.W. Sun, J.Y. Baek, K.H. Kim, et al., Chem. Mater. 27 (2015) 6675–6681.
[20] B. Li, Z. Wang, S.J. Su, et al., Adv. Opt. Mater. 7 (2019) 1801496.
[21] F.E. Held, A.A. Guryev, T. Frohlich, et al., Nat. Commun. 8 (2017) 15071.
[22] S.M. Kim, J.H. Yun, S.H. Han, et al., J. Mater. Chem. C 5 (2017) 9072–9079.
[23] B. Li, Z. Li, T. Hu, et al., J. Mater. Chem. C 6 (2018) 2351–2359.
[24] J. Guo, X.L. Li, H. Nie, et al., Chem. Mater. 29 (2017) 3623–3631.
[25] M. Liu, X.L. Li, D.C. Chen, et al., Adv. Funct. Mater. 25 (2015) 5190–5198.